

Fabrication of Nanoflowers and Other Exotic Patterns

Hardev Singh Virk

Professor Emeritus, Eternal University, Baru Sahib, HP, India
hardevsingh.virk@gmail.com

Keywords: Electro-deposition, Hydrothermal method, Anodic Alumina & Polymer templates, Nanoflowers, Exotic patterns, Nucleation rate.

Abstract. A wide variety of metallic and metal oxide nanoflowers and other exotic patterns have been fabricated using different techniques. We have created copper and cupric oxide nanoflowers using two different techniques: electro-deposition of copper in polymer and anodic alumina templates, and cetyltrimethyl ammonium bromide (CTAB)-assisted hydrothermal method, respectively. Zinc oxide and manganese oxide nanoflowers have been synthesized by thermal treatment. Characterization of nanoflowers is done in the same way as for nanowires using XRD, SEM, TEM and FESEM. Scanning Electron Microscope (SEM) images record some interesting morphologies of metallic copper nanoflowers. Field Emission Scanning Electron Microscope (FESEM) has been used to determine morphology and composition of copper oxide nanoflowers. X-ray diffraction (XRD) pattern reveals the monoclinic phase of CuO in the crystallographic structure of copper oxide nanoflowers. Nanoflowers find interesting applications in industry. There is an element of random artistic design of nature, rather than science, in exotic patterns of nanoflowers fabricated in our laboratory.

1. Introduction

During the last decade, exhaustive reviews [1-4] have been published on metal nanostructures. A series of various nanoflowers and nanoflower-like structures have been obtained, depending on reaction conditions, such as reagents ratio, temperature and other conditions. Nanoflower structure may consist of such more simple nanostructures; as nanorods, nanowalls, or nanowires. Current and possible applications of nanoflowers as optoelectronics devices or sensors, in catalysis, and solar cells caused a definite interest in them. Nanoflowers of almost all metals have been reported in the form of elemental nanoflowers; metal oxide nanoflowers; nanoflowers of hydroxides and oxosalts; sulphide, selenide and telluride nanoflowers; nitride and phosphide nanoflowers; nanoflowers formed by organic and coordination compounds [1].

Flower-like cupric oxide (CuO) nanostructures have been prepared via cetyltrimethyl ammonium bromide (CTAB)-assisted hydrothermal method [5]. CTAB is a useful surfactant that has been widely used in fabricating the nanomaterials to control the morphology. Cao et al. [6] reported CTAB-assisted hydrothermal synthesis of CuO of various morphologies such as rod-like, spheriodal, hexahedron and other irregular structures. Cupric oxide (CuO) has potential applications in many fields, such as superconductor [7], gas sensor [8], catalyst [9], magnetic storage media [10] and lithium battery [11]. Synthesis of CuO nanoflowers and their application as an H₂O₂ sensor has been reported by Gu et al. [12]. They successfully synthesized CuO nanoflowers by heating Cu(NO₃)₂·3H₂O and NH₃·H₂O for 6 h at low temperature. No additives, surfactants and templates were used in their synthesis.

Hybrid organic-inorganic nanoflowers were discovered by accident by Ge et al. [13] when they added 0.8 mM CuSO₄ to phosphate buffered saline (PBS) containing 0.1 mg/ml bovine serum albumin (BSA) at pH 7.4 and 25 °C. After three days, a precipitate appeared with porous, flower-like structures. Hybrid organic-inorganic nanoflowers using copper (II) ions as the inorganic component and various proteins as the organic component are being investigated for promising biosensor applications. The protein molecules form complexes with the copper ions, and these complexes become nucleation sites for primary crystals of copper phosphate. Interaction between

the protein and copper ions then leads to the growth of micrometre-sized particles that have nanoscale features and that are shaped like flower petals. When an enzyme is used as the protein component of the hybrid nanoflower, it exhibits enhanced enzymatic activity and stability compared with the free enzyme. This is attributed to the high surface area and confinement of the enzymes in the nanoflowers.

Copper phthalocyanine nanoparticles and nanoflowers have been investigated by Karan et al. [14]. Metal phthalocyanines (MPcs) are very well known dye pigments having similarity in structure with biological molecules chlorophyll and haemoglobin. These materials have shown many interesting properties and high vacuum evaporation has become the most widely used technique for the deposition of MPc films [15–18]. Attempts have been made to use such films as molecular components in a number of electronic and optoelectronic devices [19–21]. For the better technological applications of phthalocyanines as organic semiconductors, electronically active organic molecules and components for molecular electronics it is necessary to study, under various experimental conditions, the interactions of these molecules with various electrode materials like gold, silver etc. As among the metal substituted phthalocyanines, copper (II) phthalocyanine (CuPc) has been found to have superior properties [22–24].

Author's group [25–30] has reported fabrication and characterization of copper nanowires and some exotic patterns of polycrystalline copper recently using electrodeposition technique of template synthesis. (CTAB)-assisted hydrothermal method [5] has also been exploited for synthesis of CuO nanoflowers. A comprehensive investigation is planned to exploit the industrial applications of copper nanoflowers, for example, field emission properties.

2. Experimental Investigations

There are several different methods for fabrication of nanoflowers as reported in various reviews [1–4]. We followed two different routes for preparation of copper nanoflowers: electro-deposition technique using template synthesis and CTAB-assisted hydrothermal method.

Electro-deposition technique used in our experiments [25–30] is similar in principle to that used for the electroplating process and has been vividly described in the Chapter on Nanowires. Commercially available polycarbonate membranes (Sterlitech, USA) of 25 mm diameter with pore density of 10^8 pores/ cm² and pore diameter of 100 nm were selected for this experiment. The main purpose of this experiment was to fabricate nanowires of copper. However, to our utter surprise, we failed in our mission and what we got was a blessing in disguise. We observed formation of some exotic patterns, including synthesis of nanoflowers.

A second set of experiments was completed using commercial anodic alumina membranes (AAM) (anodisc 25 made by Whatman) having an average pore diameter of 200 nm, a nominal thickness of 60 μ m and a pore density of 10^9 pores/cm², as templates.

The electrochemical cell, fabricated in our laboratory using Perspex sheets, was washed in double distilled water. A copper rod of 0.5 cm diameter was used as a sacrificial electrode (anode). The cathode consists of copper foil attached to polymer template by an adhesive tape of good conductivity. The electrolyte used had a composition of 20 gm/100ml CuSO₄.5H₂O + 25% of dilute H₂SO₄ at room temperature. The inter-electrode distance was kept 0.7 cm and a current of 2mA was applied for 10 minutes. After electrodeposition, the polymer template was dissolved in dichloromethane to liberate copper nanoflowers from the host matrix. Copper nanowires were produced generally using AAM template but in some cases, nanoflowers appeared on the periphery of template due to poor contact. The Scanning Electron Microscope (JEOL, JSM 6100) was used to record top and side views of grown nanostructures at an accelerating voltage of 20kV using different magnifications.

For hydrothermal synthesis [5], analytical grade (Loba Chemicals) copper chloride dihydrate, $\text{CuCl}_2 \cdot 2\text{H}_2\text{O}$, and sodium hydroxide, NaOH, were used as precursors and CTAB as surfactant. All the chemicals were directly used without further purification and de-ionized water was used for preparation of solution.

In a typical synthesis, the copper chloride solution was prepared by dissolving 0.85g (5mmol) of $\text{CuCl}_2 \cdot 2\text{H}_2\text{O}$ in 20 mL de-ionized water. Subsequently, the copper chloride solution was slowly dropped into 50mL of NaOH solution (3mol.L^{-1}) under vigorous stirring. The blue-colored precursor was obtained. 1g of CTAB (3 mmol) was added to the blue-colored precursor and stirred vigorously for 30 min at 50°C to ensure the complete dissolution of CTAB. This reaction solution was then transferred to a 50 mL Teflon-lined stainless steel autoclave and heated at 150°C for 12 h in an electric oven. After reaction, autoclave was allowed to cool to room temperature. The resulting black precipitate was centrifuged and washed thoroughly with de-ionized water and ethanol. Then the precipitate was dried in drying oven at 50°C for 24 h. Finally, the reaction products were calcined in a furnace at 500°C for 2h in an ambient air atmosphere.

Among metal oxides, ZnO has been most investigated and its morphologies usually include nanowires, nanorods, nanobelts, nanorings, nanosheets, nanodisks, nanoflowers, nanoneedles, nanonails, nanopencils, and nanoflakes [31-33]. As another important application of ZnO nanoflowers, a new amperometric biosensor for hydrogen peroxide was developed [34]. Rapid response, expanded linear response range, and excellent stability were found for this biosensor. Flower-shaped ZnO nanostructures composed of ZnO nanosticks have been synthesized by the solution process followed by thermal treatment by Wang et al. [35].

Synthesis of ZnO nanoflowers was carried out by solution process at 180°C using zinc acetate dihydrate, sodium hydroxide and PEG-20000 as source materials. For the synthesis, equivalent volume zinc acetate dihydrate (0.5M) and sodium hydroxide (5M) were mixed to obtain solution A. 1g PEG-20000 was dissolved in 4 ml of water by sonication to obtain solution B. The solution B was then added into 5 ml solution A to obtain solution C. 55 ml of 1-octanol was added to solution C under stirring at room temperature to obtain solution D. Then solution D was transferred to Teflon-lined stainless steel autoclave which was then heated at 180°C for 4 h in an electric oven. The ZnO white powder could be obtained after filtering, washing and drying. The mechanism of flower-shaped ZnO formation is illustrated (Fig. 1). SEM images of ZnO nanoflowers are also shown (Fig. 2) [35]. The X-ray diffraction pattern of synthesized ZnO powder confirmed that the ZnO nanoflowers conform to wurtzite hexagonal structures. More detailed information about ZnO nanoflowers is reported elsewhere [36-40]. SEM image of ZnO teterapods is shown in figure 3 [41].

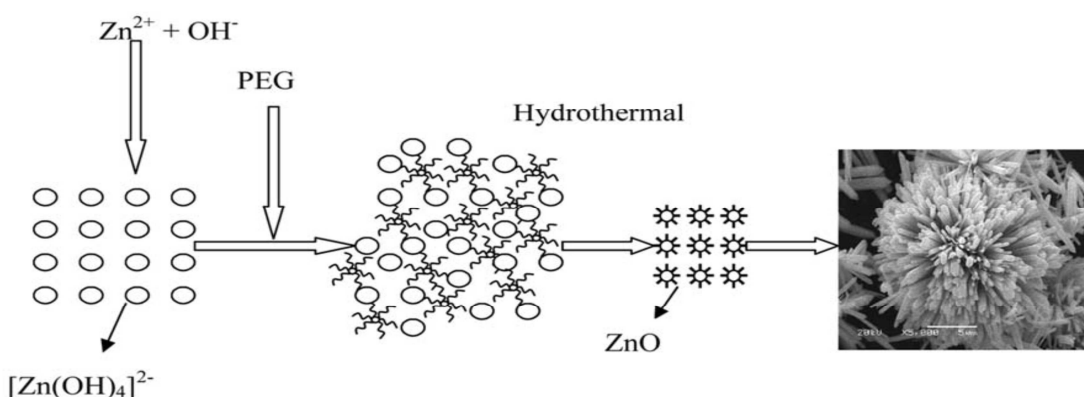


Fig. 1 Illustration of the formation mechanism of flower-shaped ZnO [35]

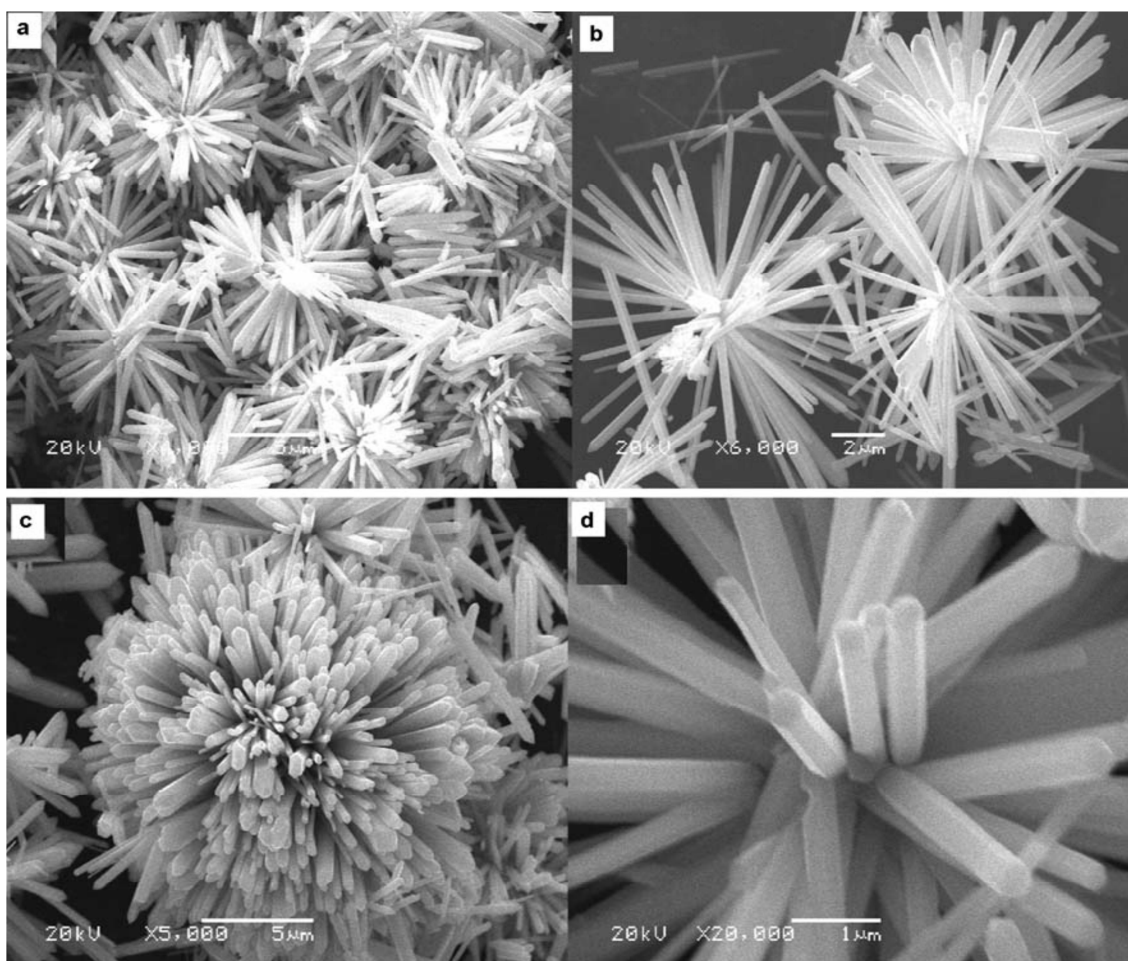


Fig. 2 SEM images of ZnO nanoflowers: (a, b) represents overall morphology, and (c, d) the detailed magnified view of an individual flower [35]

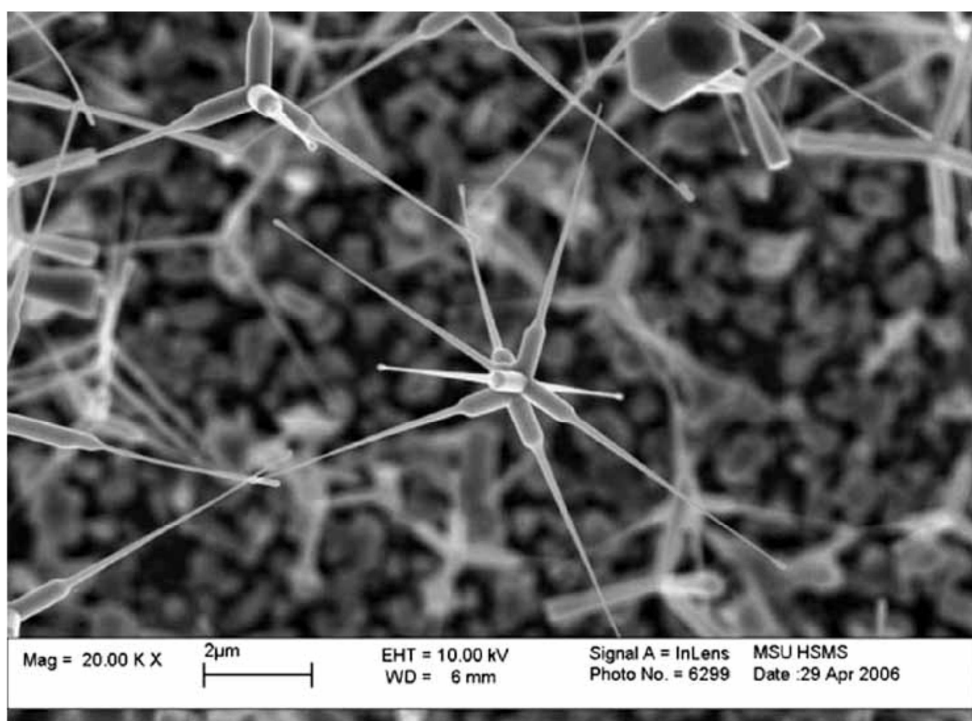


Fig. 3 SEM image of ZnO tetrapods (snowflakes) [41]

Synthesis of MgO nano-structures production by chemical vapor transport and condensation, with its distinct nanoforms could be obtained [42]. Single crystalline MgO nanoflowers, consisting of MgO nanofibers (20-80 nm), were synthesized via conventional evaporation method using the high-purity magnesium powders and distilled water as starting materials [43]. The obtained MgO nanoflowers have a much higher relative dielectric constant as compared with MgO micropowders and may be useful in providing insight into the formation of microbiological systems and reinforcing composite materials. The different steps of formation mechanism of MgO nanoflowers have been discussed by Fang et al. [44] and it includes Mg particles formation on the Si substrate, formation of MgO clusters as nucleation centers on the magnesium melt surface and the nucleation of short MgO nanofibers, and then the growth of the MgO nanofibers into MgO nanoflowers (Fig. 4).

Elegant three-dimensional MoS₂ nanoflowers (Fig. 5), consisting of tens to hundreds of hexagonal petals (100-300 nm wide and several nm thick) and exhibiting excellent field emitter properties, were uniformly formed via heating a MoO₂ thin film formed on a Mo foil in a sulphur vapor atmosphere at 950-1000 °C [45]. Hydrothermal synthesis leads to different MoS₂ morphologies, in particular nanoflowers at much longer aging period [46].

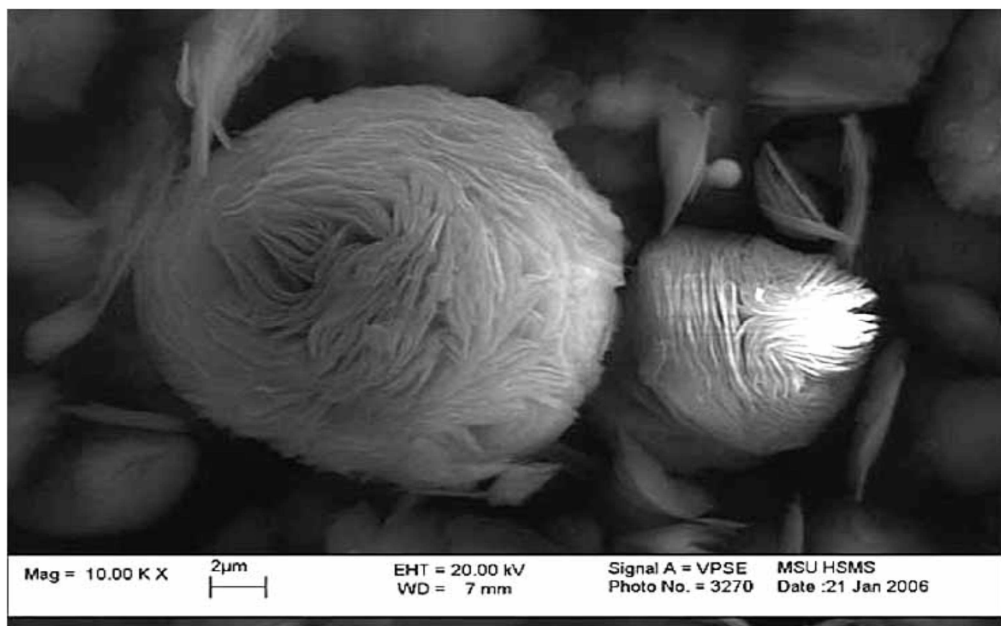


Fig. 4 SEM Image of Mg (OH)₂ nanoroses [41]

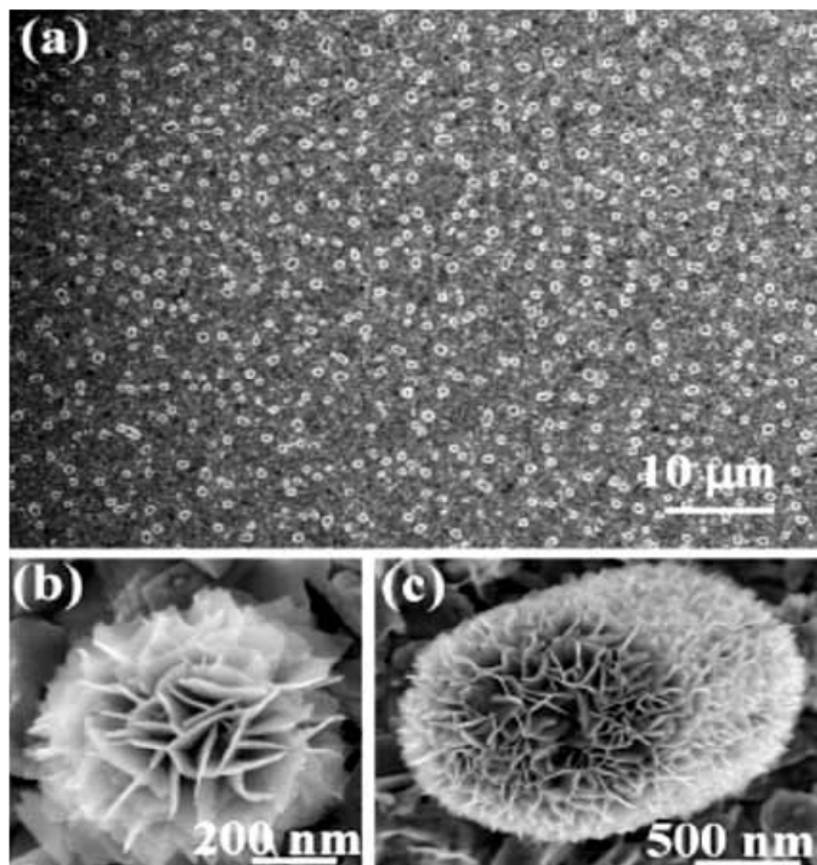


Fig. 5 SEM images of MoS₂ flower-like nanostructures: **(a)** low magnification view; **(b, c)** high magnification view [45]

Crystalline GaP nanoflowers (Fig. 6) with cubic structure composed of numerous GaP nanowires were synthesized through heating InP and Ga₂O₃ powders [47]. The authors proposed that GaP nanoflowers may be valuable for future nanodevice design. Similar nanoflower-like GaP nanostructures, constituted also by numerous nanowires (diameters of 80-300 nm; lengths varying from several to tens of μ ms), were fabricated by another route: through the close-spaced vapor transport technique (CSVt) by growing on crystalline GaAs, using a GaP powder source in the absence of any catalyst [48].

For the synthesis of the protein–inorganic hybrid nanoflowers, 20ml of aqueous CuSO₄ solution (120 mM) in molecular-biology-grade water was added to 3 ml of PBS (pH 7.4) containing proteins with different concentrations, followed by incubation at 258 °C for three days. For SEM analysis, the suspension of the prepared nanoflower was filtered and dried on a membrane (pore size, 0.1mm) and sputter-coated with gold. For TEM analysis, a drop of the suspension of the prepared nanoflower was added to a carbon grid and dried at room temperature. Figure 7 shows the SEM images of hybrid nanoflowers at different protein concentrations.

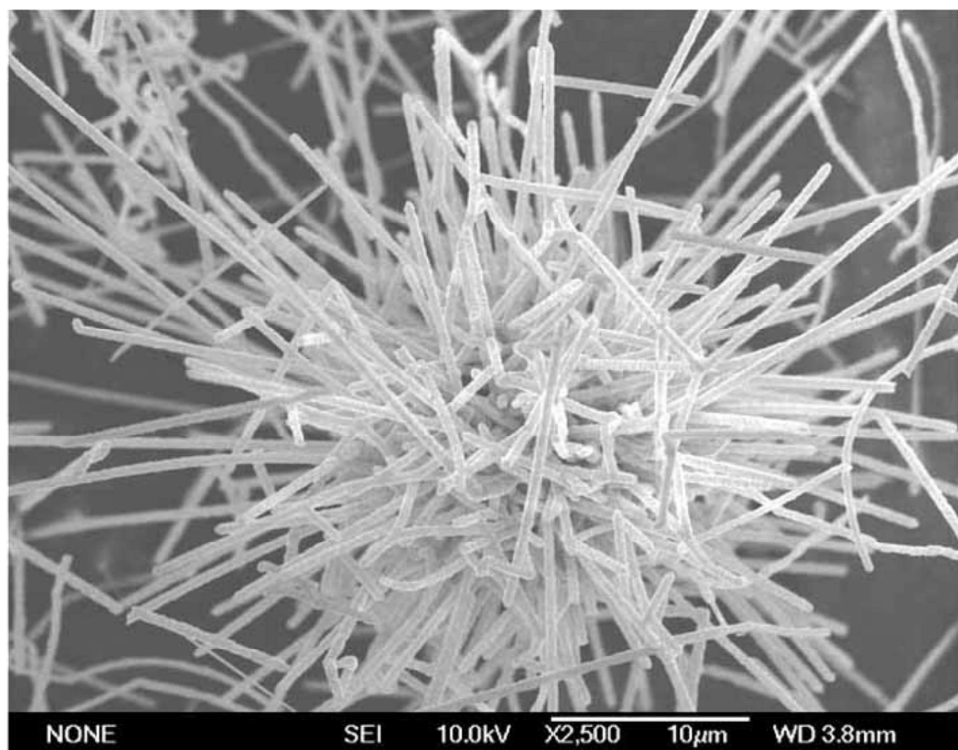


Fig. 6 SEM image of GaP nanoflowers [47]

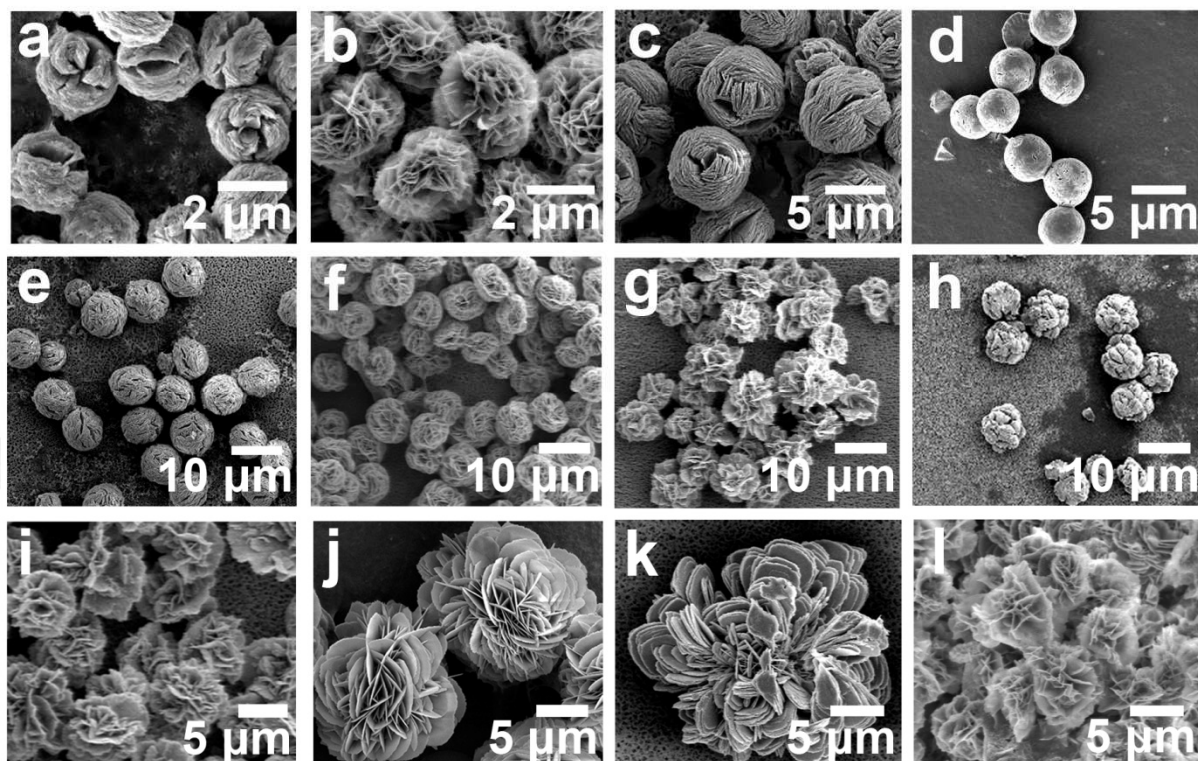


Fig. 7 SEM images of hybrid nanoflowers. Column 1 (from left to right): α -lactalbumin, column 2: laccase, column 3: carbonic anhydrase, and column 4: lipase, at protein concentrations of 0.5 mg/mL (**a-d**), 0.1 mg/mL (**e-h**), and 0.02 mg/mL (**i-l**). From this figure, the morphological changes with concentration conditions are clearly evident [adopted from ref. 13].

Karan et al. [14] synthesized copper phthalocyanine (CuPc) nanoflowers in the following way: Gold single crystal with (111) surface orientation was used as a target. Clean gold film surfaces were prepared on the surface of clean quartz plates by D.C. sputtering (7 KV, 10 mA) for 4 min followed

by annealing for 1 h at 500 °C and 750 °C under vacuum. The substrates annealed at 500 °C and 750 °C are referred to as Au-500 and Au-750, respectively. The CuPc source contained in a molybdenum boat was resistively heated in the high vacuum chamber. The CuPc powder (β form, dye content about 97%, obtained from Aldrich, USA) was used after repeated degassing of the source prior to deposition. Deposition was noted to occur when the chamber pressure could no longer reduce to the base pressure and the current through the boat was kept constant at 20 A. CuPc films were deposited at a chamber pressure of 10 Torr. The thickness of the deposited CuPc film and the rate of deposition were maintained at 100 nm and 0.6 Å/s, respectively using a quartz crystal microbalance (Hitech, model DTM-101). The temperature of the substrates during deposition was kept at room temperature (30 °C).

FESEM images of CuPc thin films deposited at room substrate temperature are shown in Fig. 8. Fig. 8(d) shows one nanoflower of diameter around 850 nm. The flower consists of some nanoribbons of CuPc of diameter nearly 25 nm and few nanometers in length. The structures of such nanoflowers arise due to the interaction of CuPc molecules with annealed gold template (Au-750), which was the same type of surface having spherical and elliptical particles of various sizes. The initial nucleation of CuPc molecules occurs at room substrate temperature on the gold particles and form flower like structure through the process of self-organization.

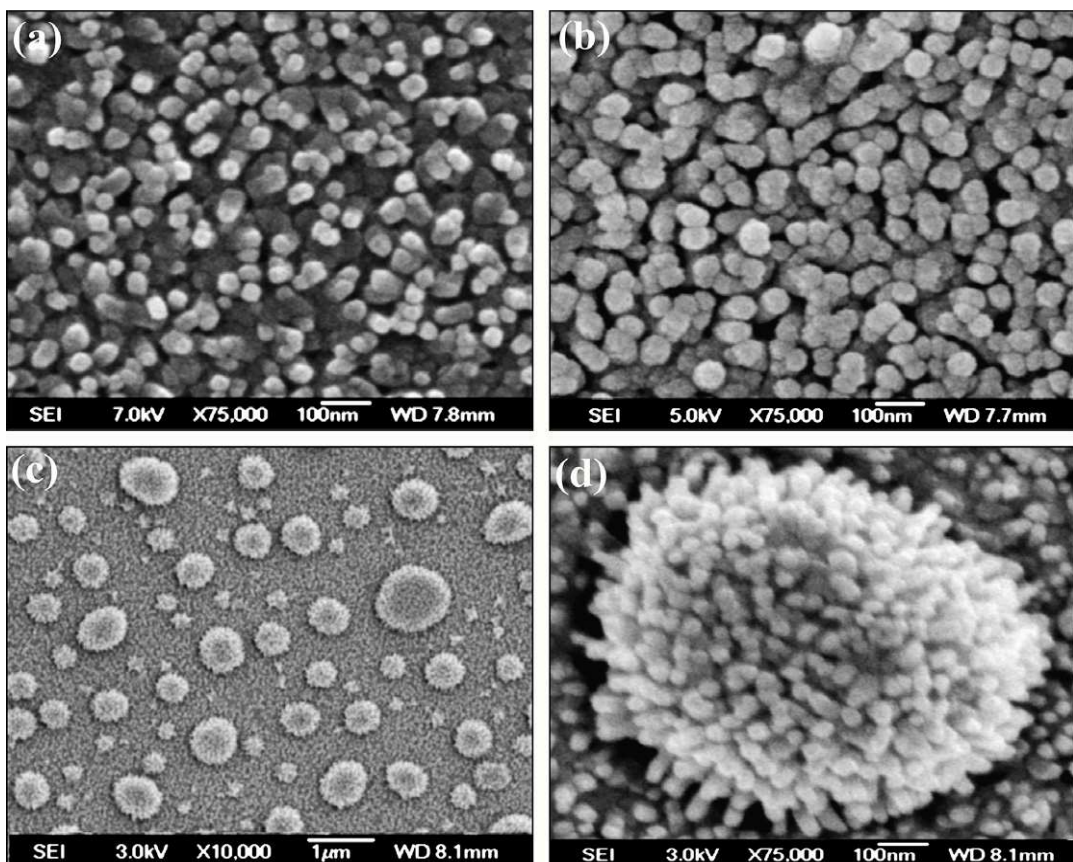


Fig. 8 FESEM images of (a) CuPc nanoparticles deposited on quartz, (b) dense and aggregated CuPc nanoparticles deposited on Au-500, (c) arrangement of spherical and elliptical CuPc nanoflowers of different sizes deposited on Au-750 and (d) CuPc nanoflower at higher magnification [adopted from ref. 14].

Chybczyński et al. [49] report for the first time on the microwave assisted hydrothermal synthesis of bismuth ferrite BiFeO_3 (BFO) nanoflowers. Bismuth ferrite, even in bulk is an unusual material because it belongs to magnetoelectric (ME) multiferroics that exhibit simultaneously

charge and magnetic ordering with some mutual coupling between them at room temperature [50-52]. These materials have recently attracted world-wide attention because of their interesting physical properties and large technological potential to be applied in spintronic devices, and in piezoelectric devices as THz radiation emitters [53].

BFO nanoflowers were synthesized by means of microwave assisted hydrothermal method using bismuth and iron nitrates as precursors: $\text{Bi}(\text{NO}_3)_3 \cdot 5\text{H}_2\text{O}$, $\text{Fe}(\text{NO}_3)_3 \cdot 9\text{H}_2\text{O}$. The nitrates together with Na_2CO_3 were added into a KOH solution of a molar concentration of 6 M. The mixture was next transferred into a Teflon reactor (XP1500, CEM Corp.) and loaded into a microwave oven (MARS 5, CEM Corp.). The reaction was carried out at the same temperature for all samples (200°C) for a short time equal to 20 min (samples labeled ST) or for one hour which was the long time synthesis (samples labeled LT). After processing, BFO powders were first cooled to 20°C , next collected by filtration kit, rinsed with distilled water and placed in a dryer for 2 h. The final products were brown powders of BFO agglomerates. In this way a set of ST and LT samples composed of grains in the shape of nanoflowers (Fig. 9) was synthesized [49].

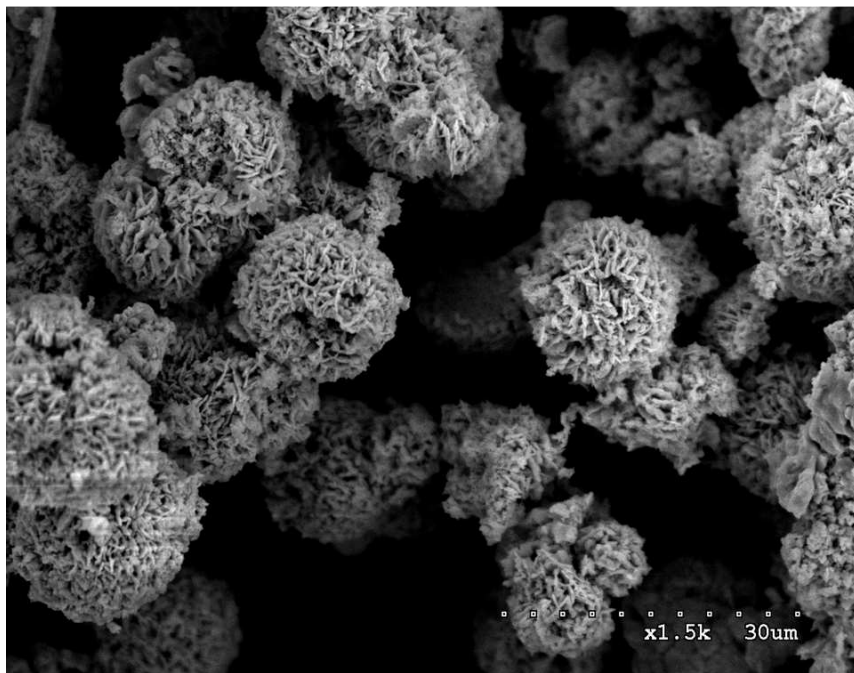


Fig. 9 SEM micrograph of bismuth ferrite (BFO) nanoflowers [adopted from ref. 49]

3. Results and Discussion

There is as yet no specific theory to explain exotic patterns developed during electro-deposition of copper in anodic alumina or polymer templates. A speculative explanation [54] is provided on the basis of over-deposition. During the growth of copper nanowires in the template pores, the current remains nearly stable until the wires arrive at the template surface. If the electro-deposition process is not stopped at this stage, the current keeps on rising very gradually leading to over-deposition of copper. The exotic patterns in the form of micro-flowers having their petals in nanometer dimension, copper buds leading to mushroom effect and double pyramid-shaped copper crystals have been observed in our investigations [25-30]. It has also been reported by National Institute of Technology (NIT), Kurukshetra [55] that over-deposition of copper in polymer templates may lead to formation of metallic micro-rose having petals in nanometer dimensions [Fig. 10]. Flower-like morphology of metal over-deposits has been attributed to the changes in hydrodynamic conditions due to excessive hydrogen evolution during electro-deposition process [55]. This explanation seems to be a tentative one which fails to justify the morphology and geometrical pattern of the flower shape formed.



Fig. 10 Copper metallic Rose flower grown in polymer template [adopted from ref. 55]

During our recent experiments, we observed that the growth of nanoflowers depends upon two factors: cathode over-potential and conductivity of the cathode surface. If the conducting film is used for the cathode surface, Cu ions will tend to deposit into nanochannels of polymer template, otherwise they tend to grow laterally on the cathode surface. The deposition of copper takes place only when the potential of the cathode is lower than the equilibrium electrode potential of the electrolytic cell; hence, a certain magnitude of cathode over-potential is necessary. The relationship between the over-potentials and the nucleation rates was given by Erdey-Gruz and Volmer [56] as follows:

$$N = a e^{-b/\eta_k^2} \quad (1)$$

where N is the nucleation rate; η_k is the cathode over-potential; a and b are constants. It can be seen that the higher the over-potential, the higher the nucleation rates of growth. At a certain optimum over-potential, nanoflower fabrication occurs.

SEM micrographs of copper nanoflowers fabricated using polymer templates are shown in Figs. 11-13. Figure 11 shows the deposition of copper in the form of flower petals. These flower petals, also called nanoflakes [57], are believed to have resulted from a nucleation process governed by an aggregation-mediated crystallization. Figure 12 depicts two different shapes of copper nanoflowers. Surprisingly, the morphology of flowers in Fig. 12 (a) is almost identical in shape and pattern but in Fig. 12 (b), it almost resembles with marigold flowers in a garden. Figure 13 represents lilly-like botanical plants of copper metal grown on the cathode surface. The beauty of these experiments is that no identical patterns are produced on repeating the experiment. It remains an enigma and defies scientific explanation.

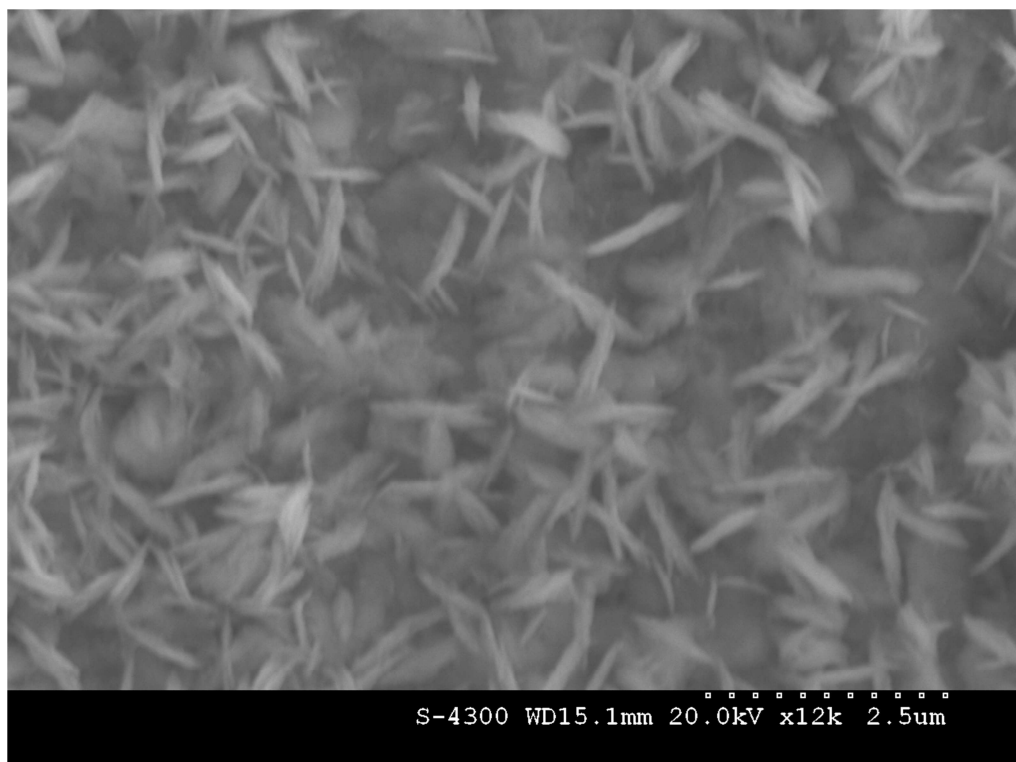


Fig.11 SEM micrograph of copper nanoflower petals grown in polymer template

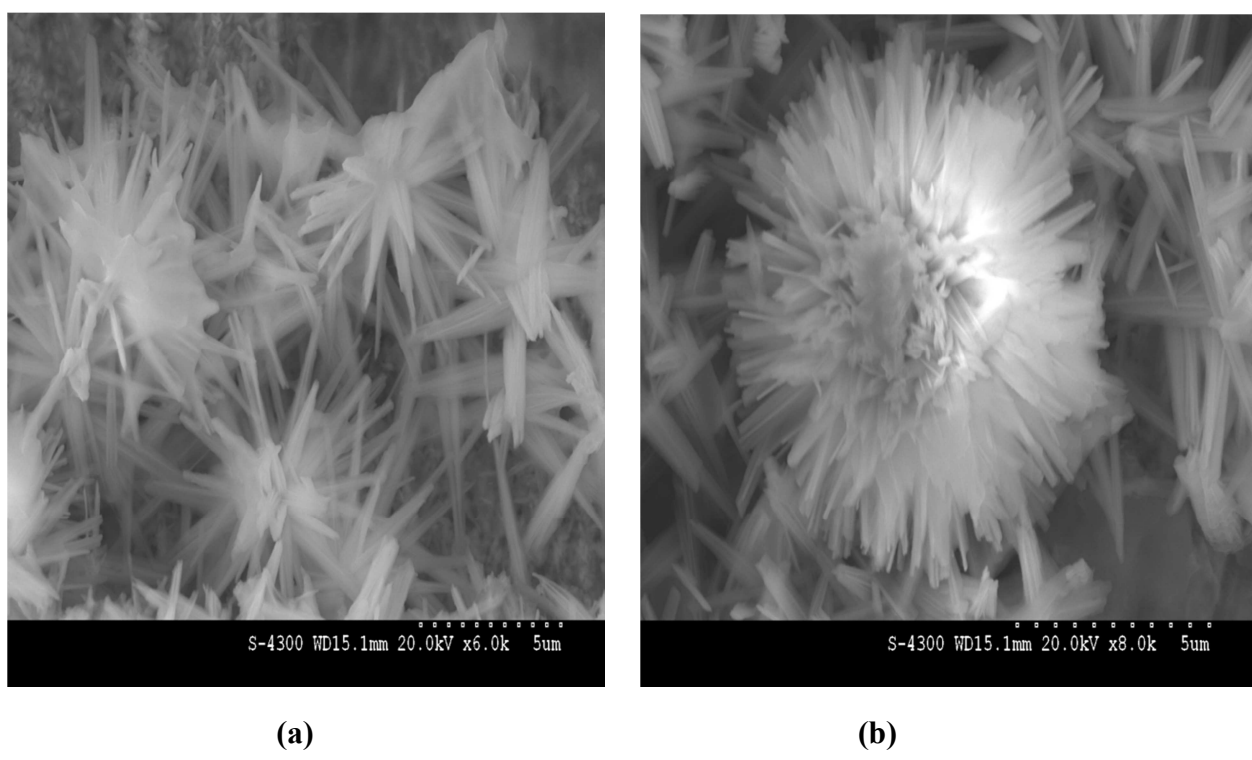
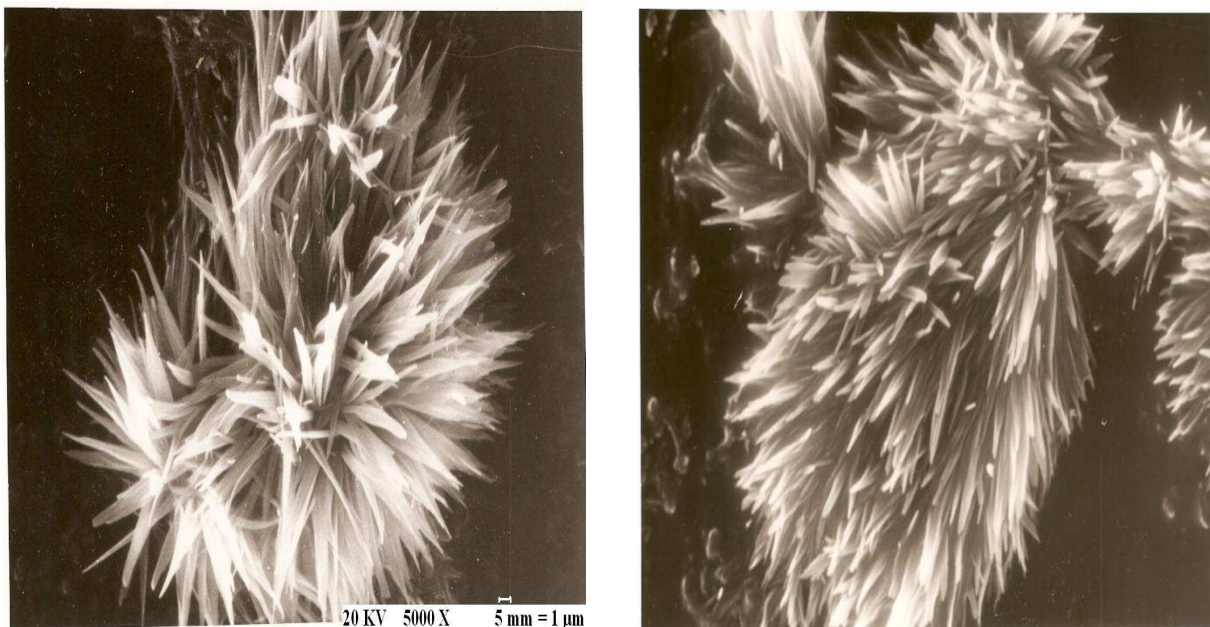


Fig. 12 (a, b) SEM micrographs of copper nanoflowers grown in polymer template

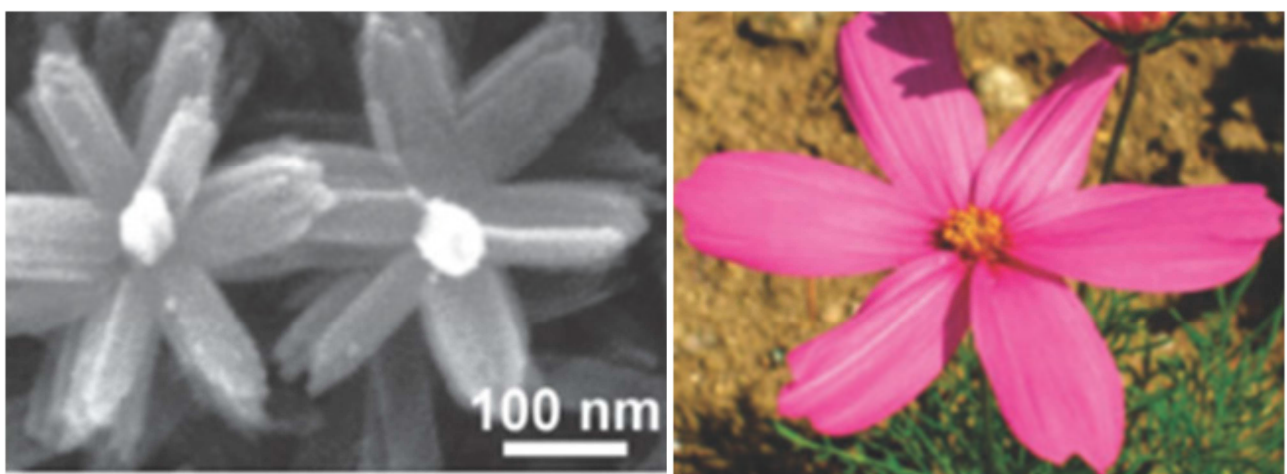


(a)

(b)

Fig. 13 (a, b) SEM micrographs of lilly-like copper plants grown in polymer template

Yang et al. [58] have found a beautiful analogy between nanoflower arrays of rutile TiO₂ and garden-cosmos (Fig. 14), as reported by Liang et al. [59] in a recent publication. The formation mechanism of rutile TiO₂ nanoflower arrays has been discussed in detail [59].



(a)

(b)

Fig. 14 (a) SEM image of rutile TiO₂ nanoflowers, and **(b)** a photograph of a garden-cosmos [58,59]

In case of anodic alumina template, copper nanowires [25] were grown in central region and nanoflowers in the peripheral zone (Fig. 15). It clearly proves the hypothesis of differential deposition of copper on the cathode surface. It is difficult to determine the exact conditions under which nanoflowers are synthesized along with nanowires. Our investigations reveal that chance plays a predominant role in growth of nanoflowers. The most disturbing feature of our study is that different types of nanostructures are created under similar experimental conditions. There is an element of random artistic design in nanoflowers fabricated in our laboratory. However, there is one satisfaction that all these exotic patterns find some analogue in nature.

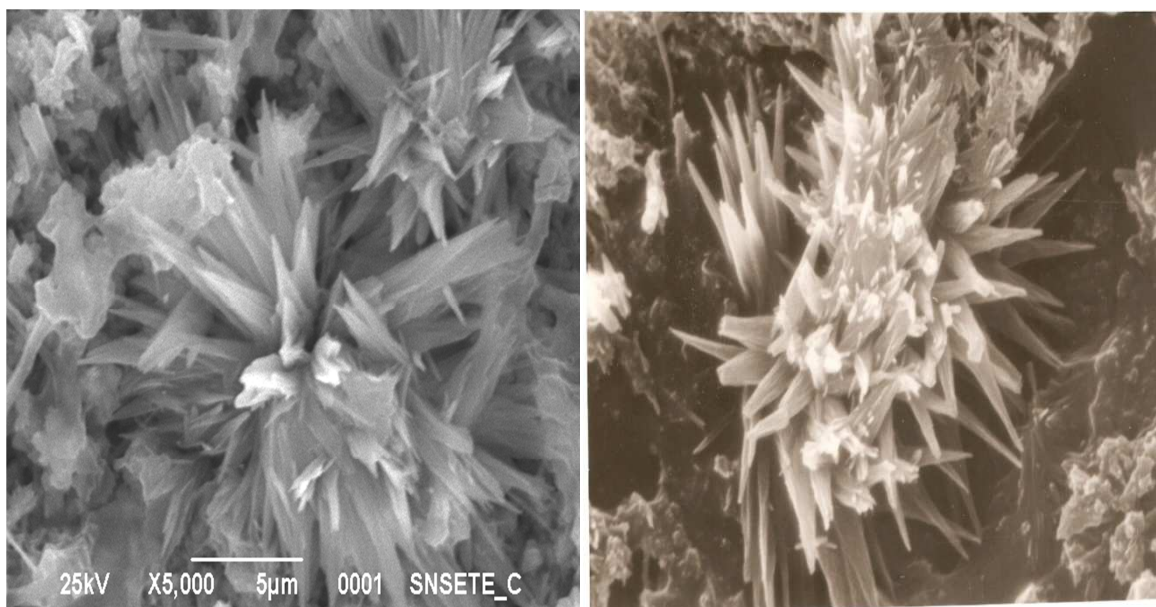


Fig. 15 (a, b) SEM micrographs of copper nanoflowers grown in anodic alumina template

It has been observed that in addition to nanoflowers, some other exotic patterns are also created during electrodeposition in anodic alumina template. An interesting feature is mushroom-like growth of copper buds of different shapes and sizes (Fig. 16). We call it the ‘Mushroom effect’. There is no specific reason for the growth of copper buds except the over-deposition of metallic copper on the cathode surface.

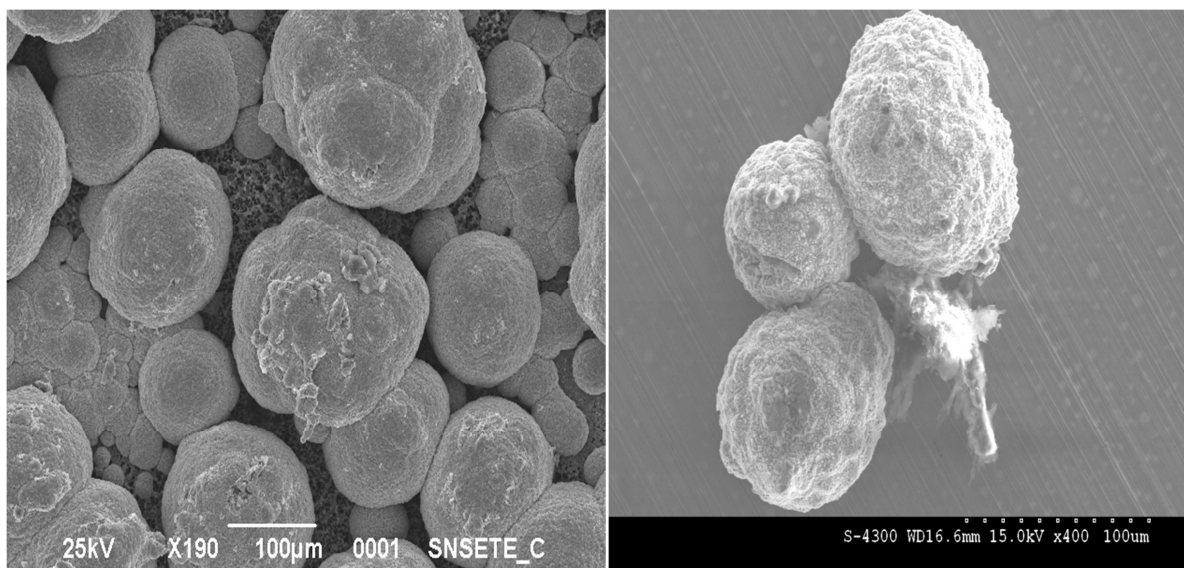
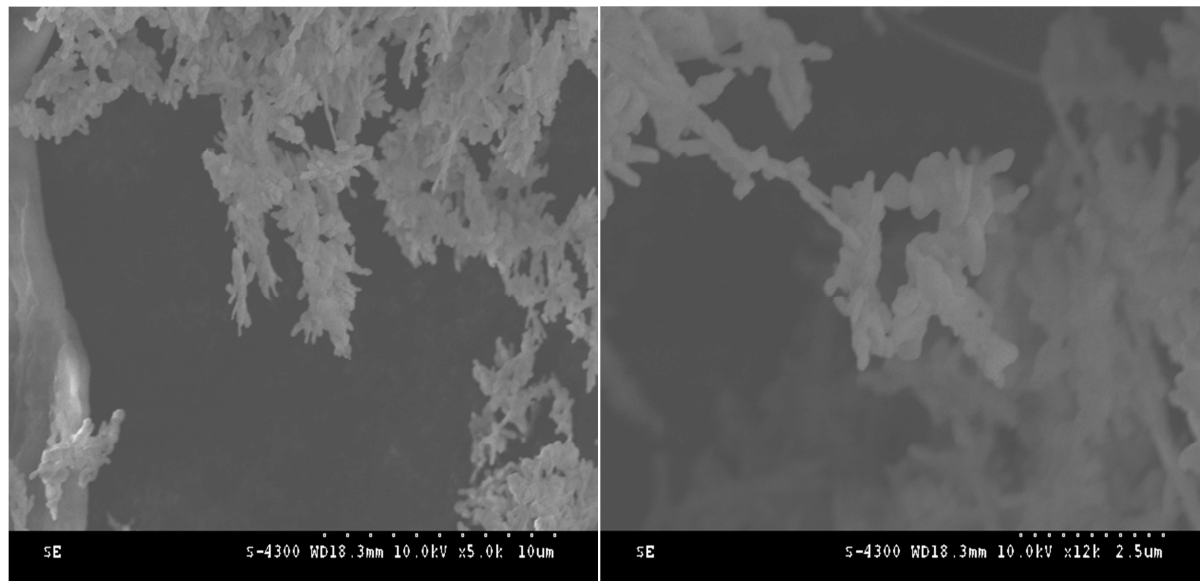


Fig. 16 (a, b) SEM micrographs of copper buds grown in alumina template (Mushroom Effect)

FESEM micrograph (Fig. 17) shows CTAB-assisted hydrothermal synthesis of CuO nanoflowers. The explanation for CTAB-assisted hydrothermal method of CuO flowers fabrication is given by Zou et al. [5]. According to the literature survey, the formation mechanisms of the flower-like CuO nanostructures were different when different preparation methods were used. Yu et al. [57] prepared the flower-like CuO nanostructures by reaction between a Cu plate and a KOH solution at room temperature and demonstrated their field emission properties. They speculated that the nanoflower was a representative morphology of spherulite formed by radiating growth from a center or a number of centers and the $[Cu(OH)_4]^{2-}$ complexes played a key role in the growth of nanoflowers.

Zhu et al. [60] used a facile chemical procedure capable of aligning CuO nanoparticles on graphene oxide and observed that the nanocomposite exhibits a high catalytic activity for the thermal decomposition of ammonium perchlorate. Teng et al. [61] synthesized the flower-like CuO nanostructures by hydrothermal process using copper threads as precursor. They investigated the influences of hydrothermal temperature and hydrothermal time on the nanostructures and reported the use of CuO as a sensor for catalysis. The formation of the flower-like structure was controlled not only by the growth thermodynamics, but also by the growth kinetics.



(a)

(b)

Fig. 17 (a, b) FESEM micrographs of CuO nanoflowers prepared by hydrothermal method

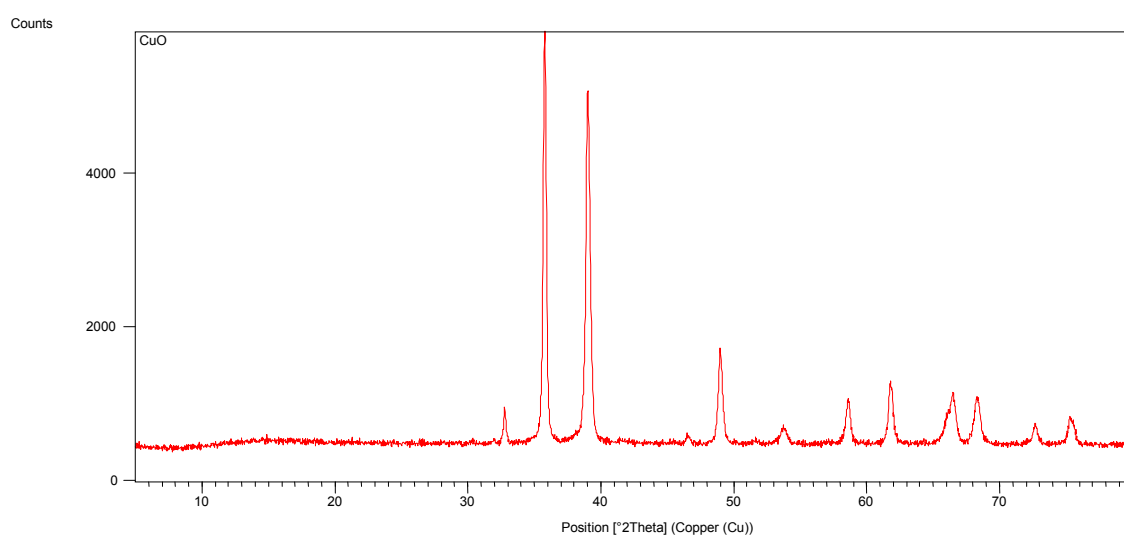


Fig. 18 XRD spectrum of monoclinic copper oxide nanoflowers

Table 1 XRD spectrum peaks data of CuO nanoflowers

Pos. [°2Th.]	FWHM [°2Th.]	d-spacing [Å]	Rel. Int. [%]	Area [cts*°2Th.]
32.7906	0.1338	2.73127	8.01	55.93
35.8066	0.2509	2.50784	100.00	1309.41
38.9983	0.1673	2.30963	83.89	732.34
46.5518	0.2676	1.95095	1.79	24.99
48.9563	0.1506	1.86061	22.75	178.74
53.7459	0.2342	1.70556	4.34	53.09
58.6036	0.3011	1.57524	10.74	168.78
61.7668	0.2007	1.50195	14.27	149.44
66.4776	0.2007	1.40649	12.33	129.17
68.2783	0.1673	1.37372	10.87	94.87
72.6435	0.3011	1.30156	4.59	72.17
75.2766	0.1632	1.26139	6.83	78.61

The crystallographic structure of copper oxide nanoflowers was investigated by X-ray diffraction analysis (XRD). The typical XRD spectrum [Fig. 18] shows 12 peaks with two major peaks at $2\theta = 35.8066$ and 38.9983 , corresponding to Miller indices (111) and (200). All the peaks are compared with the standard XRD spectrum (AMCSD Card Number: 99-101-0934 of American Mineralogist Crystal Structure Database) [62], and a perfect matching exists between the two spectra. In comparison with standard XRD spectrum, the main peak at $2\theta = 35.8066$ can be indexed to characteristic diffraction of monoclinic phase of CuO with cell parameters ($a=0.4653$ nm, $b=0.3410$ nm, $c=0.5108$ nm). The Miller indices of all the peaks in XRD spectrum are represented by (110), (111), (200), (201), (202), (112), (020), (113), (022), (220), (311) and (222), respectively, corresponding to 12 peaks in Fig. 18.

Energy dispersive X-ray analysis (EDX) of CuO nanoflowers was performed using the FESEM facility of Central Scientific Instruments Organization (CSIO), Chandigarh to determine their chemical composition and stoichiometry. The spectrum (Fig. 19) reveals 3 major peaks: two peaks of copper and one peak of oxygen. Table 2 reveals that the chemical composition of nanoflowers by weight percent and atomic percent are reciprocal. EDX spectrum reveals the chemical purity of CuO nanoflowers as other trace impurities are found to be absent.

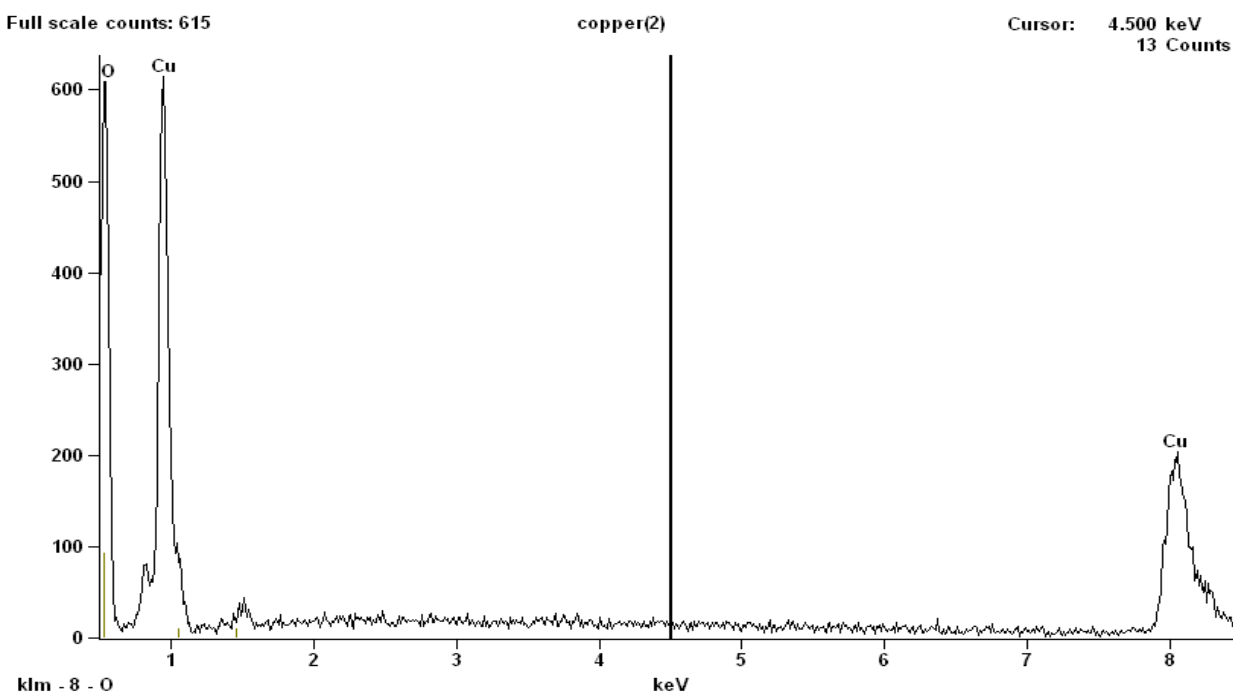


Fig. 19 EDX spectrum of copper oxide nanoflowers prepared by hydrothermal method

Table 2 Quantitative results for copper oxide nanoflowers composition

<i>Element</i>	<i>Weight %</i>	<i>Weight %</i>	<i>Atom %</i>	<i>Atom %</i>
<i>Line</i>		<i>Error</i>		<i>Error</i>
<i>O K</i>	33.60	+/- 0.73	66.77	+/- 1.44
<i>Cu K</i>	66.40	+/- 3.31	33.23	+/- 1.66
<i>Total</i>	100.00		100.00	

During the present series of experiments, our aim was to investigate the phenomenon of growth of nanoflowers and exotic patterns instead of copper nanowires. For this purpose, we used both sputter coated and as received anodic alumina templates (AAT) of 100 nm pore diameter. In case of unspattered, or as received templates, we observed synthesis of polycrystalline copper crystals (Fig. 20a), copper buds acting as nucleation centers for nanowires (Fig. 20b) and copper nanoflowers (Fig. 21) grown on the cathode surface when alumina template was dissolved in 1 M NaOH for 1 hour in a beaker under gentle shaking. These flower shapes have nothing in common with those of figures 12 and 13, grown in polymer templates. Surprisingly, when the experiment was repeated using sputter-coated alumina template of 100 nm pore diameter with a thin film of copper, the growth of nanorods of identical shape was observed in abundance (Fig. 22).

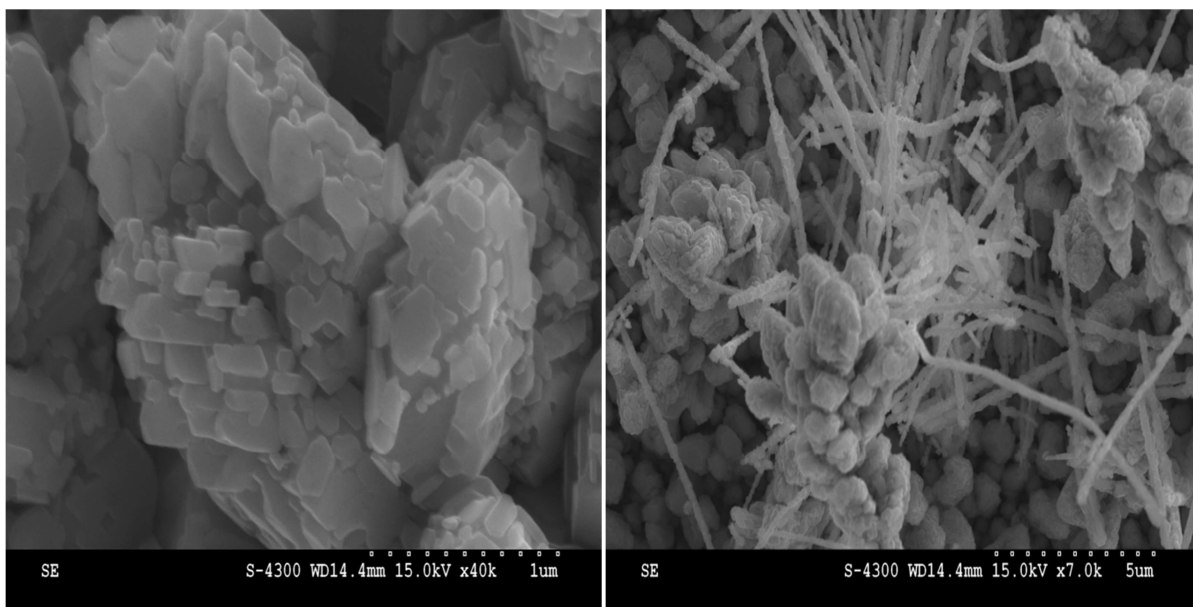


Fig. 20 (a, b) SEM micrographs showing growth of copper crystals and nanowires

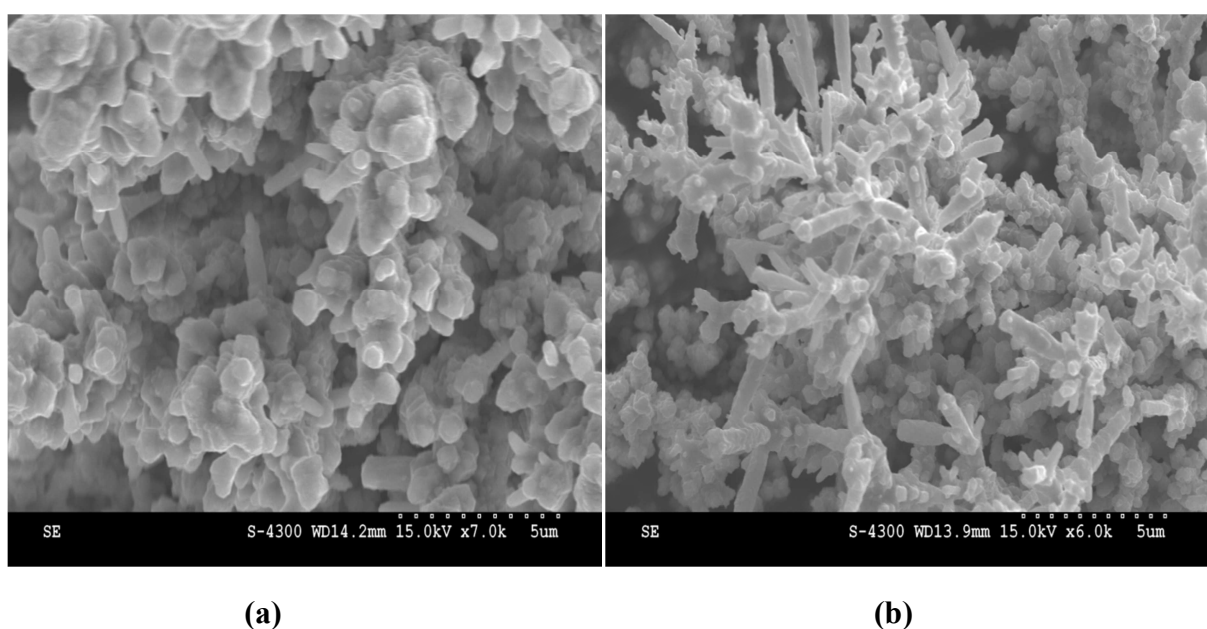


Fig. 21 (a, b) SEM micrographs of copper nanoflowers grown in AAT of 100 nm pore diameter

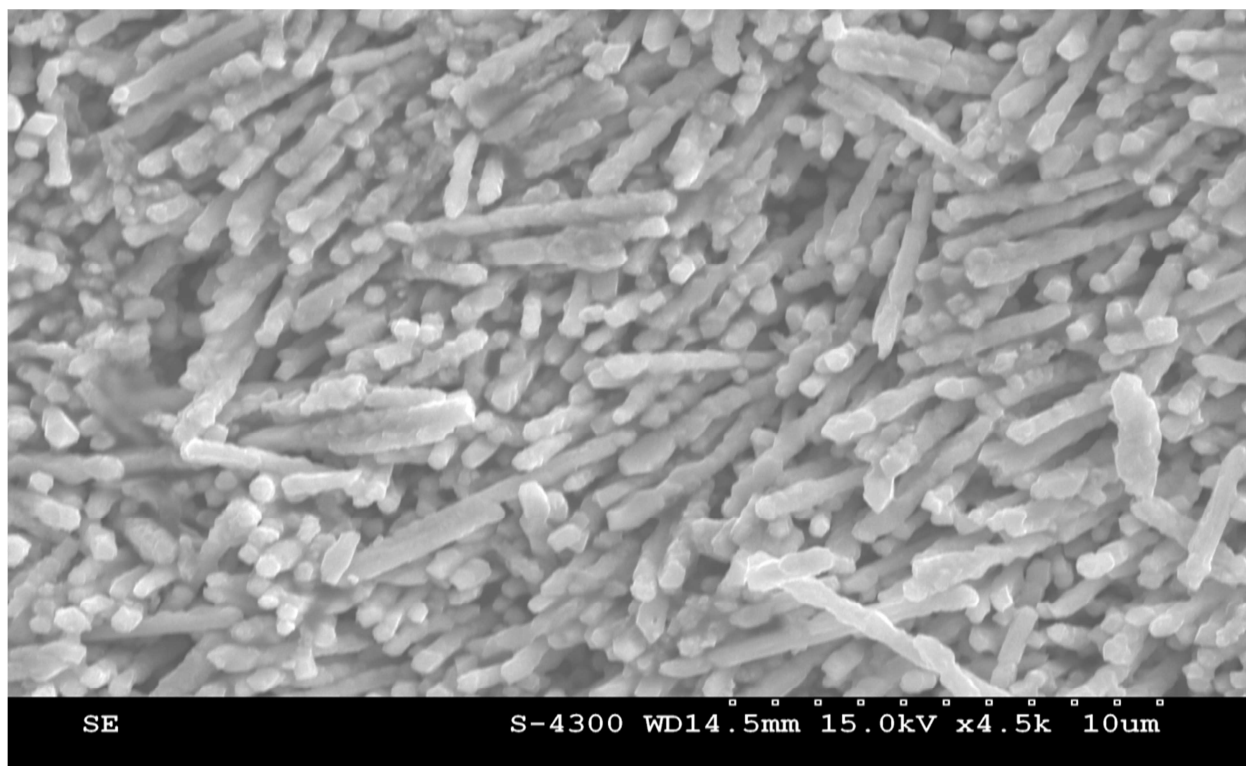


Fig. 22 SEM micrograph of copper nanorods grown in AAT of 100 nm pore diameter

In the case of anodic alumina template (AAT), it was also observed that if the template is not sputter-coated with a conducting film, the copper nanowires were synthesised in the central region and nanoflowers in the peripheral zone [25].

4. Summary

Template synthesis is an elegant method for fabrication of copper nanoflowers, using anodic alumina or polymer templates. Over-deposition plays a key role in the growth of exotic patterns of copper. It is difficult to determine the exact conditions under which nanoflowers are synthesized along with nanowires. It shows differential deposition of copper on the cathode surface. CuO nanoflowers prepared by CTAB-assisted hydrothermal method, exhibit monoclinic phase and polycrystalline nature. No scientific theory is yet available to explain their exact nature. It has been discovered that nanoflowers have great potential for possible applications in nanotechnology. CuO nanoflowers have been exploited as sensor for hydrogen peroxide (H_2O_2) [12, 63] and glucose [64], as well as for field emission properties [65]. Carbon nanotube-wired ZnO nanoflowers have been used as hydrazine sensors [58]. ZnO nanoflowers are finding application in solar cells [66], and ZnO bifunctional nanoflowers loaded with gold nanoparticles show enhanced conversion efficiency in solar cells [67].

References

- [1] B.I. Kharisov, Recent Patents on Nanotechnology, 2 (3) (2008) 190-200.
- [2] O.V. Kharissova and B.I. Kharisov, Recent Patents on Nanotechnology, 2(2) (2008) 103-119.
- [3] O.V. Kharissova, B.I. Kharisov, T.H. Garcia and U.O. Mendez, Synthesis and Reactivity in Inorganic, Metal-Organic and Nano-Metal Chemistry, 39 (2009) 662-684.
- [4] B.I. Kharisov and O.V. Kharissova, Less-common nanostructures in the forms of vegetation, Ind. Eng. Chem. Res. 49 (2010) 11142-11160.

- [5] Y. Zou, Y. Li, N. Zhang and J. Li, Prepared of flower-like CuO via CTAB-assisted hydrothermal method, *Adv. Mater. Res.* 152-153 (2011) 909-914.
- [6] M.H. Cao, C.W. Hu, Y.H. Wang, Y.H. Guo, C.X. Guo and E.B. Wang, A controllable synthetic route to Cu, Cu₂O and CuO nanotubes and nanorods, *Chem. Comm.* 15 (2003) 1884-1885.
- [7] J.H. Schon, M. Dorget, F.C. Beuran, X.Z. Zu, E. Arushanov, C.D. Cavellin and M. Lagues, Superconductivity in CaCuO₂ as a result of field-effect doping, *Nature*, 414 (2001) 434-436.
- [8] Y. Li, J. Liang, Z. Tao and J. Chen, CuO particles and plates: Synthesis and gas-sensor application, *Mater. Res. Bull.* 43 (2008) 2380-2385.
- [9] J.B. Reitz and E.I. Solomon, Propylene oxidation on copper oxide surfaces: electronic and geometric contributions to reactivity and selectivity, *J. Am. Chem. Soc.* 120 (1998) 11467-11478.
- [10] J. Ziolo, F. Borsa, M. Corti, A. Rigamonti and F. Parmigiani, Cu nuclear quadrupole resonance and magnetic phase transition in CuO, *J. Appl. Phys.* 67 (1990) 5864-5866.
- [11] X.P. Gao, J.L. Bao, G.L. Pan, H.Y. Zhu, P.X. Huang, F. Wu and D.Y. Song, Preparation and Electrochemical Performance of Polycrystalline and Single Crystalline CuO Nanorods as Anode Materials for Li Ion Battery, *J. Phys. Chem. B* 108 (2004) 5547-5551.
- [12] A. Gu, G. Wang, X. Zhang and B. Fang, Synthesis of CuO nanoflower and its application as a H₂O₂ sensor, *Bull. Mater. Sci.* 33 (1) (2010) 17-20.
- [13] J. Ge, J. Lei and R.N. Zare, Protein-inorganic hybrid nanoflowers, *Nature Nanotech.* 7 (2012) 428-432.
- [14] S. Karan, D. Basik and B. Mallik, Copper phthalocyanine nanoparticles and nanoflowers, *Chem. Phys. Lett.* 434 (2007) 265-270.
- [15] E. Jungyo, S. Kim, E. Lim, K. Lee, D. Cha and B. Friedman, Effects of substrate temperature on copper (II) phthalocyanine thin films, *Appl. Surf. Sci.* 205 (2003) 274-279.
- [16] Y. Choe, S.Y. Park, D.W. Park and W. Kim, Influence of a Stacked-CuPc Layer on the Performance of Organic Light-Emitting Diodes, *Macromol. Res.* 14 (2006) 38-44.
- [17] I. Biswas, H. Peisert, M. Nagel, M. B. Casu, S. Schuppler, P. Nagel, E. Pellegrin, T. Chassé, Buried interfacial layer of highly oriented molecules in copper phthalocyanine thin films on polycrystalline gold, *J. Chem. Phys.* 126 (2007) 174704/1-5.
- [18] H. Peisert, I. Biswas, L. Zhang, M. Knupfer, M. Hanack, D. Dini, M. Cook, I. Chambrier, T. Schmidt, D. Batchelor, T. Chassé, Orientation of substituted phthalocyanines on polycrystalline gold: distinguishing between the first layers and thin films, *Chem. Phys. Lett.* 403 (2005) 1.
- [19] C.C. Leznoff and A.B.P. Lever, Phthalocyanines, Properties and applications, Vol.3, VCH, New York, 1993.
- [20] F. Young, M. Shtein and S.R. Forrest, Controlled growth of a molecular bulk heterojunction photovoltaic cell, *Nature Mater.* 4(1) (2005) 37-41.
- [21] R. Koshy and C.S. Menon, Effect of Vacuum Annealing on the Optoelectric and Morphological Properties of F16CuPc Thin Films, *E-Journal of Chemistry* 9(1) (2012) 294-300, <http://www.e-journals.net>.
- [22] K. Kudo, K. Shimada, K. Marugami, M. Iizuka, S. Kuniyoshi and K. Tanaka, Organic static induction transistor for color sensors, *Synth. Metals* 102 (1999) 900-903.
- [23] S.A. Van Slyke, C.H. Chen and C.W. Tang, Organic electroluminescent devices with improved stability, *Appl. Phys. Lett.* 69 (1996) 2160-2163.

- [24] J.M. Auerhammer, M. Knupfer, H. Peisert and J. Fink, The copper phthalocyanine / Au (100) interface studied using high resolution electron energy-loss spectroscopy, *Surf. Sci.* 506 (2002) 333-338.
- [25] H.S. Virk, V. Balouria and K. Kishore, Fabrication of Copper Nanowires by Electrodeposition using Anodic Alumina and Polymer Templates, *J. Nano Res.* 10 (2010) 63-67.
- [26] H.S. Virk, Fabrication and Characterization of Copper Nanowires, *J. NanoSci. NanoEngg. & Applications*, 1(1) (2011) 1-16.
- [27] H.S. Virk, Fabrication of polycrystalline copper nanowires by electrodeposition in anodic alumina membrane and their characterization, *Nano Trends* 9(1) (2010) 1-9.
- [28] H.S. Virk, Template growth of copper nanowires and exotic patterns of metallic copper using electrodeposition technique, *Int. J. of Adv. Engg. Tech. (India)* 2(3) (2011) 64-68.
- [29] H.S. Virk, Fabrication and characterization of metallic Copper and Copper Oxide nanoflowers, *Pakistan J. of Chemistry* 1(4) (2011) 1-7.
- [30] H.S. Virk, Fabrication and Characterization of Copper Nanowires, in: Abbass Hashim (Ed.), *Nanowires – Implementations and Applications*, 2011, pp. 455-470. ISBN: 978-953-307-318-7, InTech Open Publishers, Rijeka, Available from: <http://www.intechopen.com/articles/show>
- [31] C.Y. Jiang, X.W. Sun, G.Q. Lo, D.L. Kwong and J.X. Wang, Improved dye-sensitized solar cells with a ZnO nanoflower photoanode, *Appl. Phys. Lett.* 90 (2007) 263501.
- [32] T.J. Hsueh and C.L. Hsu, Fabrication of gas sensing devices with ZnO nanostructure by the low- temperature oxidation of zinc particles, *Sensors & Actuators B Chem.* 131(2) (2008) 572-576.
- [33] C. Ge, Z. Bai, M. Hu, D. Zeng, S. Cai and C. Xie, Preparation and gas-sensing property of ZnO nanorod-bundle thin films, *Mater. Lett.* 62(15) (2008) 2307-2310.
- [34] C. Li, G. Fang, N. Liu, Y. Ren, H. Huang and X. Zhao, Snowflake-like ZnO structures: Self-assembled growth and characterization. *Mater. Lett.* 62(12) (2008) 1761-1764.
- [35] J. Wang, S. Zhang, J. You, H. Yan, Z. Li, X. Jing and M. Zhang, ZnO nanostructured microspheres and grown structures by thermal treatment, *Bull. Mater. Sci.* 31 (2008) 597-601.
- [36] B. Wen, Y. Huang and J.J. Boland, Controllable Growth of ZnO Nanostructures by a Simple Solvothermal Process, *J. Phys. Chem. C* 112(1) 2008 106-111.
- [37] Z. Fang, K. Tang, G. Shen, D. Chen, R. Kong and S. Lei, Self-assembled ZnO 3D flower- like nanostructures, *Mater. Lett.* 60(20) (2006) 2530-2533.
- [38] J. Zhang, Y. Yang, B. Xu, F. Jiang and J. Li, Shape-controlled synthesis of ZnO nano- and micro-structures. *J. Cryst. Growth* 280(3) (2005) 509-515.
- [39] S-H. Jung, O. Em, K-H. Lee, et al., Sonochemical preparation of shape-selective ZnO nanostructures, *Crystal Growth Des.* 8(1) (2008) 265-269.
- [40] R. Wahab, S.G. Ansari, Y.S. Kim, et al., Low temperature solution synthesis and characterization of ZnO nano-flowers. *Mater. Res. Bull.* 42(9) (2007) 1640-1648.
- [41] Y.D. Tretyakov (Ed.), *Nanotechnologies. The alphabet for everyone (in Russian)*, Fizmatlit 2008, pp. 344-345.[42] H.Y. Feng, M.G. Wen, Z. Ye, et al., Tuning the architecture of MgO nanostructures by chemical vapour transport and condensation, *Nanotechnology* 17(19) (2006) 5006-5012.
- [43] F. Xiao-Sheng, Y. Chang-Hui Y, X. Ting, et al., Regular MgO nanoflowers and their enhanced dielectric responses, *Appl. Phys. Lett.* 88 (2006) 013101.
- [44] X-S Fang, C-H Ye, L-D Zhang, J-X Zhang, J-W Zhao and P. Yan, Direct observation of the growth process of MgO nanoflowers by a simple chemical route, *Small* 1(4) (2005) 422-428.

- [45] Y.B. Li, Y. Bando and D. Golberg, MoS₂ nanoflowers and their field-emission properties, *Appl. Phys. Lett.* 82(12) (2003) 1962-1964.
- [46] R. Wei, H. Yang, K. Du, et al., A facile method to prepare MoS₂with nanoflower-like morphology, *Mater. Chem. Phys.* 108(2-3) (2008) 188-191.
- [47] B.D. Liu, Y. Bando, C.C. Tang, D. Golberg, R.G. Xie and T. Sekiguchi, Synthesis and optical study of crystalline GaP nanoflowers, *Appl. Phys. Lett.* 86 (2005) 083107.
- [48] C. Felipe, F. Chavez, C. Angeles-Chavez, E. Lima, O. Goiz and R. Pena-Sierra, Morphology of nanostructured GaP on GaAs: Synthesis by the close-spaced vapor transport technique, *Chem. Phys. Lett.* 439(1) (2007) 127-131.
- [49] K. Chybczynska, P. Lawniczak, B. Hilczer, B. Leska, R. Pankiewicz, A. Pietraszko, L. Kepinski, T. Kaluski, P. Cieluch, F. Matelski, B. Andrzejewski, Synthesis and Properties of Bismuth Ferrite Multiferroic Nanoflowers, arXiv:1212.2538 [cond-mat.mtrl-sci] 11 Dec 2012.
- [50] M. Fiebig, Revival of magnetoelectric effect, *J. Phys. D: Appl. Phys.* 38 (2005) R123-R152.
- [51] A.M. Kadomtseva, Yu. F. Popov, A.P. Pyatakov, G.P. Vorobev, A.K. Zvezdin, D. Viehland, Phase transitions in multiferroic BiFeO₃ crystals, thin-layers and ceramics: enduring potential for a single phase, room-temperature magnetoelectric “holy grail”, *Phase Trans.* 79 (2006) 1019-1042.
- [52] D. Lebeugle, D. Colson, A. Forget, M. Viret, P. Boville, J.M. Marucco, S. Fusil, Room temperature co-existence of large electric polarization and magnetic order in BiFeO₃ single crystals. *Phys. Rev. B* 76 (2007) 024116-1-8.
- [53] G. Catalan, J.F. Scott, Physics and applications of bismuth ferrite, *Adv. Mat.* 21 (2009) 2463-2485.
- [54] T. Gao, G. Meng, Y. Wang, S. Sun and L.J. Zhang, Electrochemical synthesis of copper nanowires, *Physics: Condensed Matter*, 14 (2002) 355-363.
- [55] S. Kumar, V. Kumar, M.L. Sharma and S.K. Chakarvarti, Electrochemical synthesis of metallic micro-rose having petals in nanometer dimensions, *Superlatt. & Microstr.* 43 (2008) 324-329.
- [56] T. Erdey-Gruz and M.Z. Volmer, *Phys. Chem.* 150A (1930) 203-213.
- [57] L.G. Yu, G.M. Zhang, Y. Wu, X. Bai and D.Z. Guo, Cupric oxide nanoflowers synthesized with a simple solution route and their field emission, *J. Cryst. Growth* 310 (2008) 3125-3130.
- [58] X.F. Yang, C.J. Jin, C.L. Liang, D.H. Chen, M.M Wu and J.C. Yu, Nanoflower arrays of rutile TiO₂, *Chem. Commun.* 47 (2011) 1184-1186.
- [59] C. Liang, W. Zhao, X. Yang, M. Wu and Y. Tong, Applications of High Resolution Electron Microscopy in Structural Analysis of Nanoarrays, in: A. Méndez-Vilas (Ed.) *Current Microscopy Contributions to Advances in Science and Technology*, © FORMATEX (2012) 1271-1282.
- [60] J. Zhu, G. Zeng, F. Nie, X. Xu, S. Chen, Q. Han and X. Wang, Decorating graphene oxide with CuO nanoparticles in a water-isopropanol system, *Nanoscale* 2(6) (2010) 988-994.
- [61] F. Teng, W.Q. Yao, Y.F. Zheng, Y.T. Ma, Y. Teng, T.G. Xu, S.H. Liang, and Y.F. Zhu, Synthesis of flower-like CuO nanostructures as a sensitive sensor for catalysis, *Sensors & Actuators B*, 134 (2008) 761-768.
- [62] R.T. Downs and M. Hall-Wallace, The American Mineralogist Crystal Structure Database, *American Mineralogist*, 88 (2003) 247-250.
- [63] K. Zhang, N. Zhang, H. Cao and C. Wang, A novel non-enzyme hydrogen peroxide sensor based on an electrode modified with carbon nanotube-wired CuO nanoflowers, *Microchimica Acta* (2011), 10.1007/s00604-011-0708-y.

- [64] Jiang LC, Zhang WD (2010) highly sensitive nonenzymatic glucose sensor based on CuO nanoparticles-modified carbon nanotube electrode. Biosens Bioelectron 25:1402
- [65] Fang B, Zhang CH, Zhang W, Wang GF (2009) A novel hydrazine electrochemical sensor based on a carbon nanotube-wired ZnO nanoflower-modified electrode, Electrochim. Acta 55 (2009) 178.
- [66] Y. Jiang, X.W. Sun, S.Q. Lo, D.L. Kwong and J.X. Wang, Improved dye-sensitized solar cells with a ZnO-nanoflower photoanode , Appl. Phys. Lett. 90 (2007) 263501.
- [67] V. Dhas, S. Muduli, W. Lee, S-H. Han and S. Ogale, Enhanced conversion efficiency in dye-sensitized solar cells based on ZnO bifunctional nanoflowers loaded with gold nanoparticles, Appl. Phys. Lett. 93 (2008) 243108, <http://dx.doi.org/10.1063/1.3049131> (*3 pages*)

Functional Nanomaterials and their Applications

10.4028/www.scientific.net/SSP.201

Fabrication of Nanoflowers and other Exotic Patterns

10.4028/www.scientific.net/SSP.201.159